

## Ionic Polymer Transducers in sensing: the streaming potential hypothesis

Lisa Mauck Weiland<sup>1\*</sup> and Barbar Akle<sup>2</sup>

<sup>1</sup>*Department of Mechanical Engineering and Materials Science, University of Pittsburgh,  
204 Benedum Hall, Pittsburgh, PA 15261, USA*

<sup>2</sup>*Department of Mechanical Engineering, Lebanese American University, Byblos, Lebanon*

*(Received July 7, 2008, Accepted August 1, 2009)*

**Abstract.** Accurate sensing of mechanical strains in civil structures is critical for optimizing structure reliability and lifetime. For instance, combined with intelligent control systems, electromechanical sensor output feedback has the potential to be employed for nondestructive damage evaluation. Application of Ionic Polymer Transducers (IPTs) represents a relatively new sensing approach with more than an order of magnitude higher sensitivity than traditional piezoelectric sensors. The primary reason this sensor has not been widely used to date is an inadequate understanding of the physics responsible for IPT sensing. This paper presents models and experiments defending the hypothesis of a streaming potential sensing mechanism.

**Keywords:** ionic polymer; sensor; Ionic Polymer Transducer (IPT); Ionic Polymer Metal Composite (IPMC).

---

### 1. Introduction

Examples of sensing applications where effectiveness is highly dependent on the sensitivity of the measuring device include vibration control, health monitoring, and flow measurement (Yun *et al.* 2009). Several active materials such as piezoelectric ceramics demonstrate large electromechanical coupling. Piezoelectric materials are reliable and able to transform mechanical energy into the electrical domain. Hence piezoelectric based devices could be used as mechanical sensors. Alternatively, Ionic Polymer Transducers (IPTs) are derived from a relatively new class of active materials with superior sensing capabilities. An IPT is made of an ionomer film sandwiched between two conductive electrodes. In charge sensing mode an IPT sensor has been shown to be one order of magnitude more sensitive than traditional piezoelectric transducers (Newbury and Leo 2002). In addition, IPTs are reliable; IPTs saturated with ionic-liquids have been shown to be environmentally stable and can operate over a million cycles in open air (Akle *et al.* 2007a, Bennett and Leo 2004). Further, these compliant sensors are suitable for conformal structures and based on fabrication requirements they are cost competitive as compared to piezoceramic, MEMS, and other state-of-the-art sensors. Finally, while not a focus in the current paper, IPT devices may have potential for power harvesting due to their large generated electromechanical currents as well as chemical energy harvesting potential.

---

\*Corresponding Author, Assistant Professor, E-mail: [lmw36@pitt.edu](mailto:lmw36@pitt.edu)

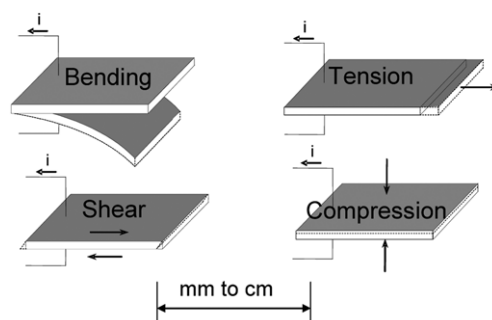


Fig. 1 IPT macroscopic sensing modes

First consider the sensing modes displayed in IPTs (Fig. 1). While sensing in the bending mode has garnered considerable attention, IPTs generate currents due to any mechanical stimulation. Moreover, IPTs generate measurable currents for extremely small deformations; a  $1\text{ mm} \times 1\text{ mm}$  IPT is capable of measuring shear stresses in fluids as low as  $1\text{ Pa}$  (Etebari *et al.* 2005). The primary reason this novel class of transducers has not been employed in high sensitivity applications is an inadequate understanding of the physics responsible for IPT sensing. This knowledge gap is exacerbated by the pervasive misconception that these transducers are limited to bending response.

In order to develop the requisite understanding of the physics of IPT sensing, it is prudent to first consider the composition of the active ionomer material. Ionomers are fabricated by the addition of covalently bonded, charged pendant groups (via pendant chains) to hydrophobic ‘backbone’ polymeric chains. The addition of charged pendant groups produces regions of phase separation; nanoscale hydrophilic *clusters* of pendant groups, counterions, and solvent reside within a hydrophobic matrix. Beyond general agreement on these points, the exact morphology has been a point of debate; in fact it has been asserted that the morphology is not discernable with certainty via the characterization strategies employed to date (Paddison 2003). In the absence of a substantive morphological model, the morphology has often been described via a simplified model of spherical clusters interconnected by ion channels which promote the transport of counterions through the polymer, or *selective ionic conduction* (Fig. 2).

Selective ionic conduction is the basis of using ionomers as polymer fuel cell membranes as well as electromechanical transducers. A fuel cell employs an ionomer membrane to convert chemical

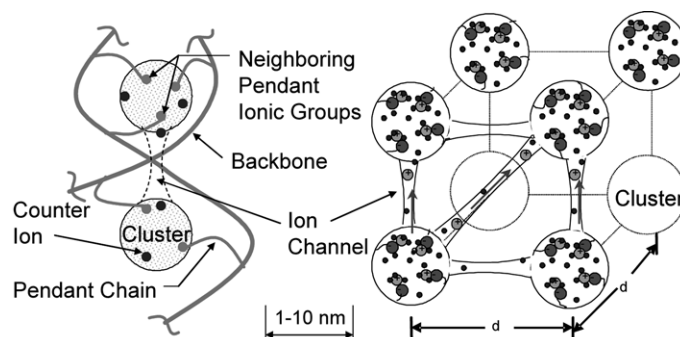


Fig. 2 Ionomer component map (left) and idealized morphology (right). Selective ionic conduction through ion channels enables electromechanical and chemoelectrical energy conversion

energy into electrical energy through selective ionic conduction of protons. This process is gaining acceptance as a means of clean energy conversion for stationary, mobile, and portable power sources (See for instance McGrath and Zawodzinski 2005). Similarly, mechanical deformation of an ionic polymer produces ionic reorganization and conduction; this produces measurable charge flow. This is the basis for use of ionomeric materials as electromechanical sensors.

Early ionomer research demonstrates that these films can be used as accelerometers for vibration sensing (Oguro *et al.* 1992, Sadeghipour *et al.* 1992). Shahinpoor *et al.* (1998) summarize research in the use of ionomeric membranes as displacement and velocity sensors, primarily through the analysis and testing of cantilever membranes. Their work quantifies the sensitivity of ionomeric materials under a variety of loading conditions.

More recently the mechanical sensing properties of ionomers have been quantified and compared to that of piezoelectric films (Newbury and Leo 2002, Farinholt and Leo 2004). These works demonstrate that ionomeric films have excellent charge-sensing response when subjected to mechanical loads. Using a two-port impedance model of an ionomeric material, it is demonstrated that ionomeric films produce two to three orders of magnitude more charge than a piezoelectric film of equivalent size.

The foregoing discussion illustrates the potential for application of ionomeric sensing arrays. Unfortunately, the majority of IPT research to date has focused on actuation properties. In fact, none of the models developed in the time since the report of Sadeghipour *et al.* (1992) have been successful in capturing the fundamental physics associated with IPT sensing. Empirical models that are useful for IPT engineering design have been developed (Newbury and Leo 2002, Bonomo *et al.* 2006, Kanno *et al.* 1996, Newbury and Leo 2003); these models are effective for narrow classes of actuator design. More general ‘hydraulic models’ of ion transport-induced deformation have also been proposed (Asaka and Oguro 2000, de Gennes *et al.* 2000, Tadokoro *et al.* 2001). Unfortunately, none of the hydraulic models of electromechanical transduction have been able to represent all types of experimentally-observed phenomena. Of the models intended to address the physics of sensing *in bending*, only that of Nemat-Nasser and Li (2000) has met with some success. The validity of this model hinges on the assumption that all pendant ionic groups are perfectly paired with counterions in spherical clusters (for the morphology of Fig. 2); this assumption introduces a level of continuum-type thinking which simplifies the mathematical analysis. Weiland and Leo subsequently investigated the equilibrium state of single clusters and concluded this assumption is unlikely to be reasonable in sensing. Rather, it is suggested that *non-ideal ion pairing enables sensing* (Weiland and Leo 2005a, b). Moreover, the polarization model proposed by Nemat-Nasser and Li cannot accommodate experimentally observed IPT sensing in tension, compression, or shear. Lastly, a compelling argument has recently been made for an ionomer morphology of parallel channels (Schmidt-Rohr and Chen 2008). If correct, this further discounts the polarization hypothesis.

Conversely, it has since been demonstrated that the electrode in IPTs plays a major role in transduction (Farinholt and Leo 2004, Akle *et al.* 2005, Nemat-Nasser 2002). Akle *et al.* have presented an electrode fabrication process for IPTs named the Direct Assembly Process (DAP) which permits the exploration of different electrode architectures (Akle 2005, Akle *et al.* 2007a, b). The generated peak strain in actuation is correlated with the interfacial surface area between the conductor phase and the ionomer. An experimental study employing the DAP will be presented in support of the hypothesis that the increasing sensitivity with increasing electrode surface area can be related to the mechanism of streaming potential.

## 2. The streaming potential hypothesis

The foundation of this report is the realization that ion transport in ionic polymers and the subsequent ion interaction with the electrode gives rise to an IPT's electromechanical sensitivity; the mechanism of streaming potential is proposed.

To illustrate the hypothesis, first consider IPT sensing in bending. Bending an IPT will result in a pressure gradient between the compressed and the expanded electrodes. This pressure gradient will be regulated by fluids flowing across the membrane carrying along the unpaired counterions. A schematic of this concept is shown in Fig. 3. The direction of the current in Fig. 3 is experimentally verified. This thought experiment is akin to that of existing hydraulic models. However, hydraulic models rely on a directional pressure gradient and therefore cannot predict a sensing response from other mechanical stimuli such as shearing or compression as illustrated in Fig. 1. With this in mind, consider next how streaming potential would manifest itself in the IPT configuration.

The electrode of an IPT is interpenetrating and interacts with the diluent of the ionomer to reach an equilibrium potential. This potential is also observed to form when a metal electrode is immersed in an electrolyte. In the latter case, this is due to the ions passing from the high chemical energy metal phase to the lower chemical energy electrolyte phase. This results in an electric double layer as illustrated in Fig. 4 (Helmholtz 1853, Gouy 1910, Chapman 1913, Stern 1924, Grahame 1947, Bockris *et al.* 1963). When the electrolyte is sheared against the electrode, it will result in a disruption of the electric double layer and generate a potential and a current in the electrode. This

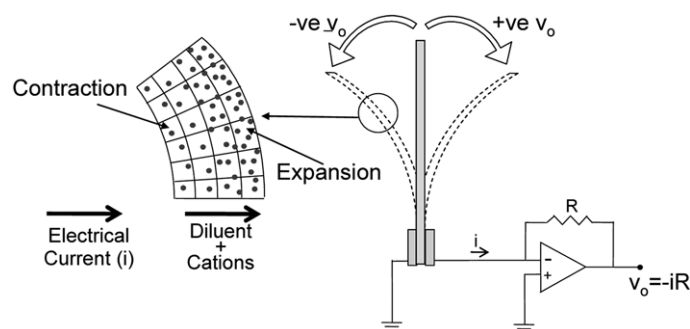


Fig. 3 Schematic of concentration difference concept

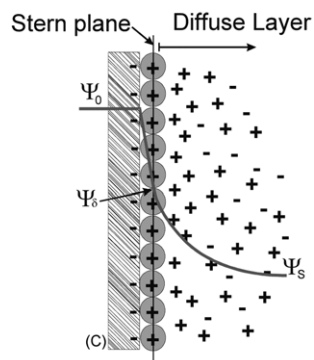


Fig. 4 Stern and Grahame representation of the electric double layer

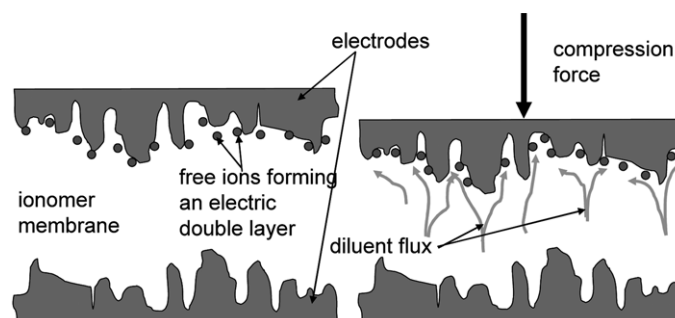


Fig. 5 Illustration of IPT streaming potential (right). The schematic illustrates the relative motion of diluent due to IPT compression

phenomenon is known as the streaming potential. Now consider that for all IPT mechanical stimuli there is a net relative motion of the electrode with respect to the electrolyte. Thus, a streaming potential develops and a current flows from the transducer. Fig. 5 shows a schematic of the relative motion due to compression of the sensor resulting in a streaming potential on the upper electrode. The figure draws attention to the importance of electrode surface area in the streaming potential hypothesis. The following experimental study illustrates the role of electrode surface area in sensing response.

### 3. Experiments

Utilizing the Direct Assembly Process (DAP), it has been demonstrated that the electrode plays a significant role in IPT transduction (Farinholt and Leo 2004, Akle *et al.* 2005, Nemat-Nasser 2002). Compared to traditional fabrication processes, the DAP allows the use of any type of ionomer, solvent, and conducting powder in the transducer, and permits the exploration of different electrode architectures.

In this study the DAP (Akle 2005, Akle *et al.* 2007a, b) is employed to fabricate six  $3\text{ mm} \times 30\text{ mm}$  transducers. The conductive particulate employed in this study is ruthenium dioxide ( $\text{RuO}_2$ ). In the case of varied electrode thickness, the electrode of each transducer is composed of 42 volume percent (vol%)  $\text{RuO}_2$  particles to Nafion<sup>®</sup> ionomer while the thickness is varied over  $10\text{ }\mu\text{m}$ ,  $25\text{ }\mu\text{m}$ , and  $40\text{ }\mu\text{m}$ . The other three samples have a constant electrode thickness of  $25\text{ }\mu\text{m}$  while the  $\text{RuO}_2$  concentration is varied over 30 vol%, 50 vol% and 60 vol%. The thickness of the middle membrane is kept constant at  $180\text{ }\mu\text{m}$  for all sensors.

One potential source of experimental error resulting from the DAP is the difficulty of precisely controlling electrode thickness. Using scanning electron microscopy (SEM), previous studies indicate approximately 10% error in the targeted thickness (Akle *et al.* 2007a). The wide variation in the thickness (from  $10\text{ }\mu\text{m}$  to  $40\text{ }\mu\text{m}$ ) and in the concentration of particles (from 30% to 60%) lowers the effect of the fabrication error on the reported performance trends.

The sensing performance is measured for each of the samples using the experimental configuration illustrated in Fig. 6. A mechanical shaker pushes the tip of the polymer and a laser micrometer measures the displacement. The applied displacement is a sine wave of 1 Hz frequency and approximate magnitude of 2 mm. The current generated due to the imposed strain is measured using

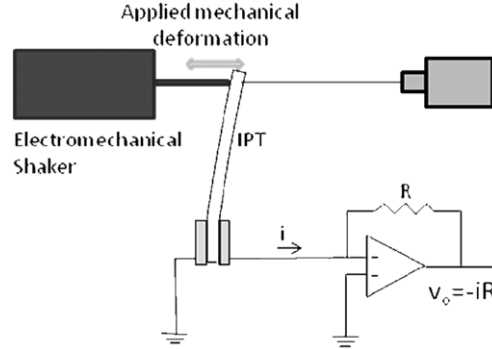
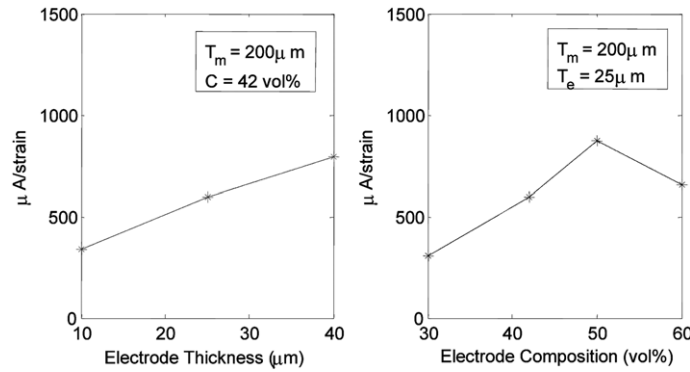


Fig. 6 Experimental configuration

Fig. 7 The normalized sensing response per unit strain of an RuO<sub>2</sub> based IPT as a function of (a) electrode thickness and (b) electrode metal composition (volume percent)

the short circuit current sensing circuit also shown in Fig. 6. The bending strain is calculated from the tip displacement according to

$$\varepsilon(t) = \frac{\delta(t)h}{L_f^2} \quad (1)$$

where  $\delta(t)$  is the measured tip displacement,  $h$  is the total thickness of the polymer and  $L_f$  is the free length of the polymer (In this study it is approximately 22 mm).

As illustrated in Fig. 7(a), increasing electrode thickness results in a linear increase in measured current per strain. In the case of varied electrode architecture, the sensing response increases from 400  $\mu\text{A}/\text{strain}$  at 30 vol% particulate up to 880  $\mu\text{A}/\text{strain}$  at 50 vol% particulate, however, there is an upper bound on this effect (Fig. 7(b)). When the metal particulate concentration is further increased to 60 vol% the sensing response drops to 700  $\mu\text{A}/\text{strain}$ . This indicates that the role of electrode communication both with itself and the remaining ionomer represents an important parameter.

#### 4. Defending the hypothesis

It is commonly accepted that the morphology of an ionomer has a strong influence on its conduction properties (Yeager and Kipling 1979). Early models of common ionomers, such as Nafion<sup>®</sup> (DuPont),

were based on the concept of ‘ion clusters’ connected by ‘ion channels’ (Hsu and Gierke 1982). These models were used to predict the ordering of the clusters and as a rationale for (as opposed to prediction of) selective ion transport in fuel cell applications (Datye *et al.* 1984, Datye and Taylor 1985). These simple morphological models have generally been regarded as incorrect, but utilized because of (1) their simplicity and (2) the absence of a generally accepted alternative. Recently, compelling arguments have been made for a parallel channel morphology (Schmidt-Rohr and Chen 2008). The parallel channel model will therefore be employed in the modeling defense of the streaming potential hypothesis. However unlike the polarization hypothesis, the validity of the streaming potential hypothesis is comparatively insensitive to the assumed morphology. Arguments to this affect will be offered at the close of this section.

To begin, consider that it has been argued that non-ideal ion pairing occurs within the ionomer (Weiland and Leo 2005a, b). The unpaired counterions are therefore distributed within the diluent and free to move, analogous to an electrolyte solution. Conversely, the negatively charged ions are covalently bonded to the surrounding hydrophobic matrix, and therefore unable to move with fluid flow. For a morphological configuration of locally parallel channels Fig. 4 may be regarded as a half-section of an individual channel. Provided flow is induced in the channel a streaming current will also be induced. In order for such a current to be displayed by the IPT as a whole, the streaming current must interact with the electrode. This model therefore considers only those channels that are in direct communication with the electrode, disregarding those in the intermittent space (‘Inactive Ionomer Region’ of Fig. 8).

It should be noted that the parallel channel morphological model (Schmidt-Rohr and Chen 2008) focuses attention on the intermittent space rather than disregarding it. In that case the locally parallel regions are also nearly parallel with each other due to processing. While the material properties resulting in a *locally* parallel configuration continue to exist in the IPT electrode region (namely, the helical nature of the polymer backbone), there is no reason to expect the regions to align with each other. Fig. 8 therefore illustrates locally parallel channels in the electrode region that are otherwise randomly oriented amongst the electrode particulates. A pressure driven flow profile within any given

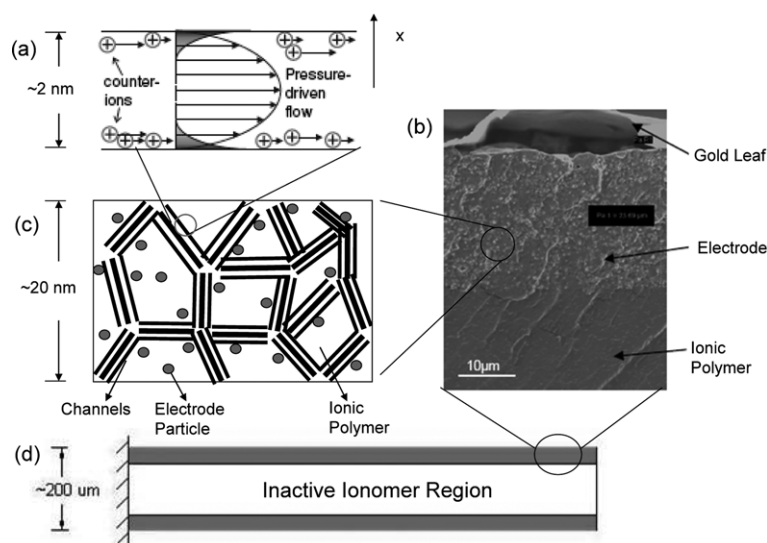


Fig. 8 Streaming current modeling construct (Not to scale)

channel, consistent with sensing in bending, is illustrated where the channels are approximately 2.5 nm in diameter. A preliminary model of this case has recently been presented in which the channels are treated as rectangular in cross section (Gao and Weiland 2008). The primary contribution of the preliminary study is its consideration of the Debye length in nanochannel flow and subsequent justification of the use of Daiguji's theory of streaming potential in nanochannels (Daiguji *et al.* 2004, van der Heyden *et al.* 2005). The streaming current can therefore be represented as

$$I_s = \int_0^R \sigma_e(r) v(r) r dr \quad (2)$$

where  $\sigma_e$  is charge density at the shear plane,  $v$  is the flow velocity of the 'electrolyte' diluent with respect to the solid electrode particulates and integration is performed with respect to the radial component of the channel cross section. In order to explore the implications of Eq. (2) for an IPT sensor  $\sigma_e$  is treated as essentially constant, leaving the need to develop an expression for  $v$ . As illustrated in Fig. 3, the velocity expression may be developed based on the pressure differential

$$v(r) = \frac{\Delta p}{4\eta l} (R^2 - r^2) \quad (3)$$

per the assumption of Poiseuille flow where  $R$  is channel radius,  $\Delta p$  is the pressure differential driving flow in bending,  $\eta$  is the fluid viscosity, and  $l$  is the length of a typical nanochannel. As described in the Experiments section, IPT sensors are typically characterized in a cantilever configuration with a load  $P$  at the free end inducing bending, thereby enabling the direct implementation of the classic beam expression  $\sigma = My/I$  (with  $\sigma_{max}$  at  $M = PL$ ). The stress expression may be used to extract the first stress invariant (or hydrostatic stress) for substitution for  $\Delta p$  in Eq. (3). The resulting expression for flow velocity within a single channel becomes

$$v(r) = \frac{M\Delta y}{3I} \frac{1}{4\eta l} (R^2 - r^2) \quad (4)$$

Where  $M$  is the moment in the vicinity of a given channel,  $I$  is the transducer's moment of inertia,  $y$  is the distance from the IPT neutral axis, and  $\Delta y$  denotes the range of consideration (to be set to the projection of channel length  $l$  aligned with the direction of flow). Substituting this expression into Eq. (2) results in a predicted streaming current of

$$I_s = \frac{\sigma_e M R^4 \cos \alpha}{48 \eta l} \quad (5)$$

where  $\alpha = 0$  corresponds with a channel completely aligned with the flow direction. A simple summation over all channels  $n$  within the electrode region provides a projection of the streaming current available for the IPT as a whole

$$I_{s, IPT} = \sum_n \frac{\sigma_e M R^4 \cos \alpha}{48 \eta l} \quad (6)$$

Per this assessment, the streaming current for an IPT with linearly increasing electrode thickness is predicted to display linear increase in the streaming current. *This is consistent with the experimentally determined response illustrated in Fig. 7(a).*

However, if the electrode thickness is held constant while the architecture is varied both the



effectiveness of electrode communication and the channel radius  $R$  are expected to vary. While the former is clearly a critical term, the fact that another parameter must also be significant is expected based on the observation of diminishing returns past a certain optimum volume fraction of particulate (Fig. 7(b)). The fact that the latter ( $R$ ) is expected to vary arises from a shifted balance of the elastic, electrostatic, osmotic, and surface energy terms which govern channel size. It is therefore prudent to explore the impact of a variable channel radius.

One approach to address the changing channel radius is via Eshelby micromechanics; this development for the specific case of a matrix with directional properties is beyond the scope of this paper. However, in general it is expected that, for otherwise consistent properties, the radius will decrease with increasing particulate volume fraction. In order to quantifiably capture this a detailed micromechanics approach for predicting the size of *spherical* inclusions will be employed (Li and Nemat-Nasser 2000) given by

$$r_c^3 = \frac{\gamma \langle h^2 \rangle M_e (\Delta V + \Delta V')}{2 N_A k T \rho_d} \left[ 1 - \sqrt[3]{\frac{4 \pi \rho_d}{3 \rho^* (\Delta V + \Delta V')}} \right] \quad (7)$$

where  $r_c$  is the radius of the spherical cluster,  $\gamma$  is the cluster surface energy density,  $\langle h^2 \rangle$  is the root mean square of the crosslinking density,  $M_e$  is the equivalent weight of the ionomer,  $\Delta V$  is the volume fraction of water,  $\Delta V'$  is the volume fraction of ion exchange sites in a dry membrane,  $N_A$  is Avogadro's number,  $k$  is the Boltzmann constant,  $T$  is the absolute temperature,  $\rho_d$  is the ionomer dry density, and  $\rho^*$  is the effective density of the wet membrane. For a given ionomer, the parameters that are subject to change as the volume fraction of electrode particulate is changed are  $\rho^*$ ,  $\Delta V$  and  $\Delta V'$ . In this study these parameters are varied per the rule of mixtures where the density of the ruthenium dioxide particulate is 7.05 g/cm<sup>3</sup>; all other values conform to those appropriate to Nafion<sup>®</sup> 1200 EW. Table 1 summarizes the resulting predictions. The second column summarizes the effect on predicted cluster radius where relative cluster size is predicted to shrink as expected; because of the geometrical differences between the spherical morphology and the cylindrical morphology imposed here, only the trend (or ratio) is of importance. Thus  $R$  in Eq. (6) is replaced by  $\beta R$ .

Consider next that the streaming current must successfully communicate with the electrode. For 0% particulate, there is no electrode, and thus there is no chance of the signal being relayed. As particulate volume fraction increases the probability of a channel being in communication with some particulate increases. For sparse distributions (such as 30 vol%), it is clear that consideration should also be given to the probability of that particulate being in communication with the electrode as a whole. For the sake of simplicity this is captured via squaring the volume fraction, with one multiplier for channel communication and one for generalized particulate communication. This would also be true for the case of increasing electrode thickness, but is constant among the points

Table 1 Predicted variation in channel size with electrode particulates and resulting impact on streaming current

RuO <sub>2</sub> volume fraction ( $v_f$ )	Radius ratio ( $\beta = R_c/R_{c,0\%}$ )	Streaming current factor ( $v_f^2 \beta^4$ )
0%	1	0
30%	0.98	0.08
40%	0.92	0.12
50%	0.85	0.13
60%	0.75	0.11

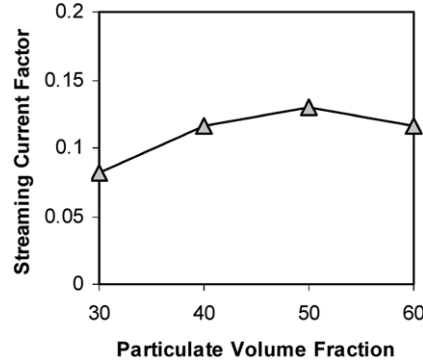


Fig. 9 Predicted streaming current trend with respect to electrode particulate volume fraction

being considered. Introducing both of these effects to Eq. (6) results in

$$I_{s, IPT} = \sum_n \frac{v_f^2 \beta^4 \sigma_e MR^4 \cos \alpha}{48 \eta l} = v_f^2 \beta^4 \cdot const \quad (8)$$

Fig. 9 illustrates the projected effect on streaming current due to varying electrode particulate volume fraction. As compared to the experimental results of Fig. 7(b) and despite the relatively simplistic state of the model, the trend is consistent with experiment.

It is next prudent to consider whether the streaming current modeling construct has the potential to project the generation of a signal for other modes of deformation. Unlike the bending mode for which there is ample validation data, the following is not a detailed assessment. Rather it is presented simply to argue that the streaming current model is capable of projecting sensing for other modes of deformation.

For the cases of tension and compression of Fig. 1, the uniaxial stress term developed due to the external load may be employed to develop the first stress invariant. This hydrostatic stress value may be substituted for  $\Delta p$  in Eq. (3); this results in the prediction of flow. Unlike the case of bending, there is not a well defined direction of pressure drop, and thus not all flow will contribute to the generation of a net current; a detailed assessment explicitly including the role of boundary conditions will ultimately be required. However, it can be reasonably argued that (1) flow within the channels will occur and (2) in both the tensile and compressive cases the upper electrode moves relative to the lower electrode. Treating the lower electrode as a fixed frame of reference (which is consistent with experiment) some proportion of the flow will be directed opposite the relative motion of the upper electrode (as illustrated in Fig. 5) and thus some signal should be predicted.

For the case of shear loading, there is no hydrostatic term and therefore no pressure term, thus the flow velocity must be developed more directly for substitution into Eq. (2). Turning to the elementary definition of viscosity where the fluid is suspended between 2 infinite plates, it is understood that motion of one of these plates relative to the other will result in a shear stress and subsequent flow in the fluid with a flow profile described by  $\tau = -\eta dv/dx$ . While the channel clearly does not align with the case of infinite parallel plates, the essence of this phenomenon remains. Namely, in those channels that largely align with the direction of shearing, the upper portion of the channel will induce a shear stress and subsequent flow in the enclosed fluid. Employing the average flow projected by the classic viscosity expression as a first order approximation results in the

expression for single channel streaming current of

$$I_s = \frac{\sigma_e P R^2 \cos \alpha}{2 L b \eta} \quad (9)$$

where  $P$  is the external IPT shear load,  $L$  is the IPT length, and  $b$  is the IPT thickness. It is unlikely that a more accurate closed form solution will ultimately be developed, rather computational methods will likely be required. Even so, inspection of this first order approximation reveals that the dependence on channel radius is significantly different from the pressure induced flow cases (raised to a power of 2 instead of 4). The role of the effectiveness of electrode communication is, however, expected to be similar in the two cases. Thus this first order approximation makes a strong case for the streaming current model's ability to project sensing in this mode, albeit of a significantly different functional form from the other modes of deformation.

It should next be reemphasized that the current form of the model gives simplistic treatment of the role of particulate communication. For comparison among cases with varied volume fractions of conductive particulate the volume fraction itself is treated as a factor projecting the probability of communication. A more fully developed statistical consideration should also consider particulate size and conductivity. At lower volume fractions of particulate it is expected that this communication term will dominate predicted response for the transducer as a whole, while the morphology parameters will increasingly affect response at high volume fractions. For comparison among cases with similar volume fractions of a conductive particulate, morphology parameters become increasingly important (for instance, as a function of ionomer type and preparation).

In the opening sections of this paper it was postulated that the streaming current hypothesis is relatively insensitive to the imposed morphology, which in turn has been a point of debate for some time. This is an especially important point when considering the creation of IPTs with ionomers other than Nafion<sup>®</sup>. The morphology imposed here has been recently presented and is admittedly amenable to the streaming current model. However, consider that even at the other morphological extreme, namely the simplified and frequently imposed model of Fig. 2, there exist pathways for electrolyte flow. Utilizing this alternate morphological construct would require consideration of the role of the Debye length; further, the predicted magnitude of response would certainly change. However, that flow would be induced may be argued on the same bases as the foregoing. This is in significant contrast to the hypothesis of a polarization mechanism which looks to the formation of a dipole within the spherical clusters. Moreover, neither the polarization model nor the earlier hydraulic models can accommodate the prediction of a sensing response in all modes of deformation. It is therefore proposed that the modeling construct presented here is robust, physically realistic, and for the first time offers the potential to project sensing in all modes of IPT deformation.

## 5. Conclusions

Reliable civil infrastructure sensor networks require high sensitivity. Piezoceramic sensors may be implemented with reasonable reliability for many cases. Alternatively, in charge sensing mode an IPT sensor has been shown to be an order of magnitude more sensitive than a traditional piezoelectric sensor. To date these sensors have not been widely employed due to a poor understanding of the mechanism responsible for sensing. This work proposes the mechanism of streaming potential in IPT sensing. The analysis and experiments suggest that the volume fraction of conductive particulate

as well as the local morphology of the ionomer play important roles in sensing response. It is also argued that the streaming potential hypothesis, unlike previous models, is able to project sensing for any mode of deformation. Full exploration of the implications of the mechanism of streaming potential will enable optimization, and ultimately reliable utilization of IPTs for sensing in any mode of deformation.

## Aknowledgements

Support for this work by NSF Career CMMI 0747123 and in part by NSF CMMI 0652937 is gratefully acknowledged.

## References

- Akle, B.J. (2005), *Characterization and modeling of the ionomer-conductor interface in ionic polymer transducers*, Ph.D. Dissertation, Virginia Polytechnic Institute and State University.
- Akle, B.J., Bennett, M., Leo, D.J., Wiles, K.B. and McGrath, J.E. (2007a), "Direct assembly process: a novel fabrication technique for large strain ionic polymer transducers", *J. Mater. Sci.*, **42**(16), 7031-7041.
- Akle, B.J., Hickner, M.A., Leo, D.J. and McGrath, J.E. (2005), "Correlation of capacitance and actuation in ionomeric polymer transducers", *J. Mater. Sci.*, **40**, 3715-3724.
- Akle, B.J., Nashwin, S. and Leo, D.J. (2007b), "Reliability of high-strain ionomeric polymer transducers fabricated using the novel direct assembly process", *Smart Mater. Struct.*, **16**(2), S256-S261 (<http://www.iop.org/EJ/abstract/0964-1726/16/2/S09/>).
- Asaka, K. and Oguro, K. (2000), "Bending of polyelectrolyte membrane platinum composites by electric stimuli Part II. Response kinetics", *J. Electroanal. Chem.*, **480**, 186-198.
- Bennett, M.D. and Leo, D.J. (2004), "Ionic liquids as stable solvents for ionic polymer transducers", *Sensor. Actuat. A-Phys.*, **115**(1), 79-90.
- Bonomo, C., Fortuna, L., Giannone, P., Graziani, S. and Strazzeri, S. (2006), "A model for ionic polymer metal composites as sensors", *Smart Mater. Struct.*, **15**(3), 749-758.
- Bockris, J.O.M., Devanathan, M. and Müller, K. (1963), "On structure of charged interfaces", *Proc. R. Soc. Lon. A.*, **274**, 55-79.
- Chapman, D. (1913), "A contribution to the theory of electrocapillarity", *Philos. Mag.*, **25**, 475-481.
- Daiguji, H., Yang, P., Szeri, A.J. and Majumdar, A. (2004), "Electrochemomechanical energy conversion in nanofluidic channels", *Nano Lett.*, **4**(12), 2315-2321.
- Datye, V.K., Taylor, P.L. and Hopfinger, A.J. (1984), "Simple model for clustering and ionic transport in ionomer membranes", *Macromolecules*, **17**, 1704-1708.
- Datye, V.K. and Taylor, P.L. (1985), "Electrostatic contributions to the free energy of clustering of an ionomer", *Macromolecules*, **18**, 1479-1482.
- Etebari, A., Akle, B.J., Bennett, M., Leo, D.J. and Vlachos, P. (2005), "A dynamic shear stress sensor for liquid environments", *Proceedings of the ASME 2nd International Symposium on Seawater Drag Reduction*, Busan, Korea, May.
- Farinholt, K. and Leo, D.J. (2004), "Modeling of electromechanical charge sensing in ionic polymer transducers", *Mech. Mater.*, **36**(5), 421-433.
- Gao, F. and Weiland, L.M. (2008), "Modeling of the electromechanical response of ionic polymer transducers by means of streaming potential mechanism", *Proceedings of the ASME SMASIS*, Ellicott City, MD, October.
- de Gennes, P.G., Okumura, K., Shahinpoor, M. and Kim, K.J. (2000), "Mechanoelectric effects in ionic gels", *Europhys. Lett.*, **50**(4), 513-518.
- Grahame, D.C. (1947), "The electrical double layer and the theory of electrocapillarity", *Chem. Rev.*, **41**(3), 441-501.

- Gouy, G. (1910), "Constitution of the electric charge at the surface of an electrolyte", *J. Phys. Radium*, **9**, 457-468.
- Helmholtz, H. (1853), "Some laws concerning the distribution of electrical currents in conductors with applications to experiments on animal electricity", *Annalen der Physik und Chemie*, **89**(6), 211-233.
- van der Heyden, F.H.J., Stein, D. and Dekker, C. (2005), "Streaming currents in a single nanofluidic channel", *Phys. Rev. Lett.*, **95**, 116104-116108.
- Hsu, W.Y. and Gierke, T.D. (1982), "Elastic theory for ionic clustering in perfluorinated ionomers", *Macromolecules*, **15**, 101-105.
- Kanno, R., Tadokoro, S., Takamori, T. and Hattori, M. (1996), "Linear approximate dynamic model of ICPF actuator", *Proceedings of the IEEE International Conference on Robotics and Automation*, Piscataway, NJ.
- Li, J.Y. and Nemat-Nasser, S. (2000), "Micromechanical analysis of ionic clustering in Nafion perfluorinated membrane", *Mech. Mater.*, **32**, 303-314.
- McGrath, J.E. and Zawodzinski, T. (2005), "Advances in materials for proton exchange membrane fuel cell systems", *Proceedings of the Asilomar Conference Grounds*, Pacific Grove, California, February.
- Nemat-Nasser, S. (2002), "Micromechanics of actuation of ionic polymer-metal composites", *J. Appl. Phys.*, **92**(5), 2899-2915.
- Nemat-Nasser, S. and Li, J.Y. (2000), "Electromechanical response of ionic polymer-metal composites", *J. Appl. Phys.*, **87**(7), 3321-3331.
- Newbury, K. and Leo, D.J. (2002), "Electromechanical modeling and characterization of ionic polymer benders", *J. Intel. Mat. Syst. Str.*, **13**(1), 51-60.
- Newbury, K.M. and Leo, D.J. (2003), "Linear electromechanical model of ionic polymer transducers part I: Model development", *J. Intel. Mat. Syst. Str.*, **14**, 333-342.
- Oguro, K., Kawami, Y. and Takenaka, H. (1992), "Bending of an ion-conducting polymer filmelectrode composite by an electrical stimulus at low voltage", *J. Micromach. Soc.*, **5**, 27-30.
- Paddison, S.J. (2003), "Proton conducting mechanisms at low degrees of hydration in sulfonic acid-based polymer electrolyte membranes", *Annu. Rev. Mater. Res.*, **33**, 289-319.
- Sadeghipour, K., Salomon, R. and Neogi, S. (1992), "Development of a novel electrochemically active membrane and 'smart' material based vibration sensor/damper", *Smart Mater. Struct.*, **1**(2), 172-179.
- Schmidt-Rohr, K. and Chen, Q. (2008), "Parallel cylindrical water nanochannels in Nafion fuel-cell membranes", *Nat. Mater.*, **7**(1), 75-83.
- Shahinpoor, M., Bar-Cohen, Y., Simpson, J.O. and Smith, J. (1998), "Ionic polymer-metal composites (IPMCs) as biomimetic sensors, actuators and artificial muscles - a review", *Smart Mater. Struct.*, **7**(6), R15-R31.
- Stern, O. (1924), "On the theory of the electrical double layer", *Z. Elektrochem.*, **30**, 508-516.
- Tadokoro, S., Takamori, T. and Oguru, K. (2001), *Modeling of IPMC for design of actuation mechanisms, Electroactive Polymer Actuators as Artificial Muscles*, (Ed. Y. Bar-Cohen), SPIE Publishing, Bellingham, WA, USA.
- Weiland, L.M. and Leo, D.J. (2005a), "Computational analysis of ionic polymer cluster energetics", *J. Appl. Phys.*, **97**(12).
- Weiland, L.M. and Leo, D.J. (2005b), "Ionic polymer cluster energetics: computational analysis of pendant chain stiffness and charge imbalance", *J. Appl. Phys.*, **97**(12).
- Yeager, H.L. and Kipling, B. (1979), "Ionic diffusion and ion clustering in a perfluorosulfonate ion-exchange membrane", *J. Phys. Chem.*, **83**(14), 1835-1839.
- Yun, G.J., Ogorzalek, K.A., Dyke, S.J. and Song, W. (2009), "A two-stage damage detection approach based on subset selection and genetic algorithms", *Smart Struct. Syst.*, **5**(1), 1-21.